

A multi-year observation of nitrous oxide at the Boknis Eck Time-Series Station in the Eckernförde Bay (southwestern Baltic Sea)

Xiao Ma¹, Sinikka T. Lennartz^{1,2}, and Hermann W. Bange¹

¹ GEOMAR Helmholtz Centre for Ocean Research Kiel, Düsternbrooker Weg 20, 24105 Kiel, Germany

² now at ICBM, University of Oldenburg, Oldenburg, Germany

Correspondence to: Xiao Ma (mxiao@geomar.de)

Abstract. Nitrous oxide (N₂O) is a potent greenhouse gas and it is involved in stratospheric ozone depletion. Its oceanic production is mainly influenced by dissolved nutrient and oxygen (O₂) concentrations in the water column. Here we examined the seasonal and annual variations of dissolved N₂O at the Boknis Eck (BE) Time-Series Station located in Eckernförde Bay (southwestern Baltic Sea). Monthly measurements of N₂O started in July 2005. We found a pronounced seasonal pattern for N₂O with high concentrations (supersaturations) in winter/early spring and low concentrations (undersaturations) in autumn when hypoxic/anoxic conditions prevail. Unusually low N₂O concentrations were observed during October 2016–April 2017, which was presumably a result of prolonged anoxia and the subsequent nutrient deficiency. Unusually high N₂O concentrations were found in November 2017 and this event was linked to the occurrence of upwelling which interrupted N₂O consumption via denitrification and potentially promoted ammonium oxidation (nitrification) at the oxic/anoxic interface. Nutrient concentrations (such as nitrate, nitrite and phosphate) at BE are decreasing since 1980s, but oxygen concentrations in the water column are still decreasing. Our results indicate a close coupling of N₂O anomalies to O₂ concentration, nutrients and stratification. Given the long-term trends of declining nutrient and oxygen concentrations at BE, a decrease in N₂O concentration, and thus emissions, seems likely due to an increasing number of events with low N₂O concentrations.

1. Introduction

Long-term observation with regular measurement intervals can be an effective way to monitor seasonal and interannual variabilities as well as to decipher short- and long-term trends of an ecosystem, which are required to make projections of the future ecosystem development (see e.g. Ducklow et al., 2009). Recently, multi-year time-series measurements of nitrous oxide (N₂O), a potent greenhouse gas and a major threat to ozone depletion (IPCC, 2013; Ravishankara et al., 2009), have been reported from the coastal upwelling areas off central Chile (Farías et al., 2015) and off Goa (Naqvi et al., 2010), in the North Pacific Subtropical Gyre (Wilson et al., 2017), and in Saanich Inlet (Capelle et al., 2018).

36 N₂O production in the ocean is generally dominated by microbial nitrification (NH₄⁺ → NO₂⁻ →
37 NO₃⁻) and denitrification (NO₃⁻ → NO₂⁻ → N₂O → N₂). During bacterial/archaeal nitrification,
38 N₂O is produced as a by-product with enhanced N₂O production under low oxygen (O₂)
39 conditions (e.g. Goreau et al., 1980; Löscher et al., 2012). N₂O is produced as an intermediate
40 during bacterial denitrification (Codispoti et al., 2005). N₂O could be further consumed via
41 denitrification to dinitrogen, however, this process is inhibited with the presence of O₂ because
42 of the low O₂ tolerance of the enzyme involved (Bonin et al. 1989). This incomplete pathway is
43 called partial denitrification and can lead to N₂O accumulation (e.g. Naqvi et al., 2000; Farías et
44 al., 2009).

45 The oceans including coastal areas contribute ~25% of the natural and anthropogenic N₂O
46 emissions (IPCC, 2013), with disproportionately high emissions from coastal and estuarine areas
47 (Bange, 2006). N₂O emissions from coastal areas strongly depend on nitrogen inputs (Seitzinger
48 and Kroeze, 1998; Zhang et al., 2010). The increasing input of nitrogen (i.e. eutrophication) has
49 become a worldwide problem in coastal waters leading to enhanced productivity and severe O₂
50 depletion caused by enhanced degradation of organic matter (Breitburg et al., 2018; Rabalais et
51 al., 2014). The decline in O₂ concentration (i.e. deoxygenation), either in coastal waters or the
52 open ocean, might result in favorable conditions for N₂O production (Codispoti et al., 2001;
53 Nevison et al., 2003). The results of a model study by Kroeze and Seitzinger (1998) indicated a
54 significant increase of N₂O in European coastal waters for 2050. Moreover, it has been suggested
55 that N₂O production and emissions are very likely to increase in the near future, especially in the
56 shallow suboxic/anoxic coastal systems (Naqvi et al., 2000; Bange, 2006). However, model
57 projections show a net decrease in future global oceanic N₂O emission during the 21st century
58 (Martinez-Rey et al., 2015; Landolfi et al., 2017; Battaglia and Joos, 2018).

59 The Baltic Sea is a nearly enclosed, marginal sea with a very limited access to the open ocean via
60 the North Sea. The restricted water exchange with the North Sea and extensive human activities,
61 such agriculture, industrial production and sewage discharge in the catchment area led to high
62 inputs of nutrients to the Baltic Sea. As a result, the areas affected by anoxia have been
63 expanding in the deep basins of the central Baltic Sea (Carstensen et al., 2014). In order to
64 control this situation, the Helsinki Commission (HELCOM) was established in 1974 and a series
65 of measures have been taken to prevent anthropogenic nutrient input into the Baltic Sea.
66 Consequently, the nutrient inputs (by riverine loads, direct point-sources and, for nitrogen,
67 atmospheric deposition) to the Baltic Sea are declining (HELCOM, 2018a). However, the
68 number of low O₂ (i.e. hypoxic/anoxic) events in coastal waters of the Baltic Sea is increasing
69 and deoxygenation is still going on (Conley et al., 2011; Lennartz et al., 2014). The
70 deoxygenation in the Baltic Sea can affect the production/consumption of N₂O. Our group has
71 been monitoring dissolved N₂O concentrations at the Boknis Eck Time-Series Station, located in
72 Eckernförde Bay (southwestern Baltic Sea), for more than a decade. In this study, we present
73 monthly measurements of N₂O and biogeochemical parameters such as nutrients and O₂ from
74 July 2005 to December 2017. The major objectives of our study were: 1) to decipher the seasonal

75 pattern of N₂O distribution in the water column, 2) to identify short-term and long-term trends of
76 the N₂O concentrations, 3) to explore the potential role of nutrients and O₂ for N₂O
77 production/consumption, and 4) to quantify the sea-to-air N₂O flux density at the time-series
78 station.

79 **2. Material and methods**

80 **2.1 Study site**

81 Sampling at the Boknis Eck (BE) Time-Series Station (www.bokniseck.de) started on 30 April
82 1957 and, therefore, it is one of the oldest continuously operated time-series stations in the world.
83 The BE station is located at the entrance of the Eckernförde Bay (54°31' N, 10°02' E, Fig. 1) in
84 the southwestern Baltic Sea. The water depth of the sampling site is 28 m. Various physical,
85 chemical and biological parameters are measured on a monthly basis (Lennartz et al., 2014).
86 There is no significant river runoff to Eckernförde Bay. Hence, the hydrographical conditions are
87 mainly dominated by saline water input from the North Sea and less saline water from the Baltic
88 Proper, which is typical for that region. Seasonal stratification usually starts to develop in April
89 and lasts until October, during which hypoxia or even anoxia (characterized by the presence of
90 hydrogen sulphide, H₂S) sporadically occurs, as a result of restricted vertical water exchange and
91 bacterial decomposition of organic matter in the bottom water (Hansen et al., 1999; Lennartz et
92 al., 2014). Thus, BE is a natural laboratory to study the influence of O₂ variations and
93 anthropogenic nutrient loads on N₂O production/consumption.

94 **2.2 Sample collection and measurement**

95 Monthly sampling of N₂O at the BE Time-Series Station started in July 2005. Triplicate samples
96 were collected from six depths (1, 5, 10, 15, 20 and 25 m). Seawater was drawn from 5 L Niskin
97 bottles into 20 mL brown glass vials after overflow. The vials were sealed with rubber stoppers
98 and aluminum caps. The bubble-free samples were poisoned with 50 µL of a saturated mercury
99 chloride (HgCl₂) solution and then stored in a cool, dark place until measurement. The general
100 storage time before measurements of the N₂O concentrations was less than three months.

101 The static headspace-equilibrium method was adopted to measure the dissolved N₂O
102 concentrations in the vials. 10 mL helium (99.9999 %, AirLiquide, Düsseldorf, Germany)
103 headspace was created in each vial with a gas-tight glass syringe (VICI Precision Sampling,
104 Baton Rouge, LA). Samples were vibrated with Vortex (G-560E, Scientific Industries Inc., New
105 York, USA) for 20 seconds and then left for at least two hours until equilibrium. 9.5 mL
106 subsample of the headspace was subsequently injected into a GC-ECD (gas chromatograph
107 equipped with the electron capture detector) system (Hewlett-Packard 5890 Series II, Agilent
108 Technologies, Santa Clara, CA, USA), which was calibrated with two standard gas mixtures
109 (N₂O in synthetic air, 320 ppb and 1000 ppb, Deuste-Steininger GmbH, Mühlhausen, Germany
110 and Westfalen AG, Münster, Germany) prior to the measurement. The average precision of the

111 measurements, calculated as the median standard deviation from triplicate measurements, was
112 0.4 nM. Triplicates with a standard deviation of >10% were omitted. More details about the N₂O
113 measurement can be found in Kock et al. (2016). Dissolved oxygen (O₂) concentrations were
114 measured by Winkler titrations (Grasshoff et al., 1999). Nutrient concentrations were measured
115 by the Segmented Continuous Flow Analysis (SCFA, Grasshoff et al., 1999). A more detailed
116 summary of the parameters measured and methods applied can be found in Lennartz et al. (2014).

117 **2.3 Times series analysis**

118 A time-series can be decomposed into three main components, i.e. trend, cycle and residual
119 component (Schlittgen and Streitberg, 2001). We used the Mann–Kendall test and wavelet
120 analysis to detect the trend and periodical cycles in the time-series data, respectively. As for the
121 residual component, we highlight unusual high/low N₂O concentrations during 2005-2017 and
122 discuss the potential causes for these events.

123 **2.3.1 Wavelet analysis**

124 In order to decipher periodical cycles of the parameters collected at the BE Time-Series Station,
125 a wavelet analysis method was adopted. Wavelet analysis enables the detection of the period and
126 the temporal occurrence of repeated cycles in time-series data. One of the requirements for
127 wavelet analysis is a regular, continuous time-series. Since there is data missing (maximum 2
128 months in a row) in the BE time-series, due to terrible weather or the ship's unavailability,
129 missing data was interpolated from the previous and following months. Sampling time varied for
130 every month (usually 20-40 day interval), but for the statistical analysis, data was assumed to be
131 regularly spaced as the uncertainty introduced was not significant (<5%). Considering the band
132 width in both frequency and time domain, a Morlet mother wavelet with a wave number of 6 was
133 chosen (Torrence and Compo, 1998). The mother wavelet was then scaled between the
134 frequency of a half-year cycle and the length of the time-series with a stepsize of 0.25. The
135 wavelet analysis was conducted with the MatLab code by Torrence and Compo [2004]. More
136 information about the method can be found on the website
137 <http://paos.colorado.edu/research/wavelets/>.

138 **2.3.2 Mann–Kendall test**

139 Mann–Kendall test (MKT) is a non-parametric statistical test to assess the significance of
140 monotonic trends for time-series measurements. It tests the null hypothesis that all variables are
141 randomly distributed against the alternative hypothesis that a monotonic trend, either increase or
142 decrease, exists in the time-series on a given significance level α (here $\alpha=0.05$). MKT is flexible
143 for data with missing values and the results are not impacted by the magnitude of extreme values,
144 which makes it a widely used test in hydrology and climatology (e.g. Xu et al., 2003; Yang et al.,
145 2004). However, MKT is sensitive to serial correlation in the time-series. The presence of
146 positive serial correlation would increase the probability of trend detection even though no such

147 trend exists (Kulkarni and von Storch, 1995). In order to avoid this situation, data from 12
148 months were tested individually. It is assumed that there is no residual effect left from the same
149 month last year, considering that the nitrogen species are rapidly biologically cycled. The Matlab
150 function from Simone (2009) was used for the MKT.

151 **2.4 Calculation of saturation and sea-to-air flux density**

152 N₂O saturations (S_{N_2O} , %) were calculated as:

$$153 \quad S_{N_2O} = 100 \times N_{2O_{obs}}/N_{2O_{eq}} \quad (1)$$

154 where $N_{2O_{obs}}$ and $N_{2O_{eq}}$ (in nM) are the observed and equilibrated N₂O concentrations in
155 seawater, respectively. $N_{2O_{eq}}$ was computed as a function of surface seawater temperature, in
156 situ salinity (Weiss and Price, 1980) and the dry mole fractions of atmospheric N₂O at the time
157 of the sampling. Since the atmospheric N₂O mole fractions were not measured at the BE Time-
158 Series Station, atmospheric dry mole fractions of N₂O were derived from the monthly average of
159 N₂O data at Mace Head, Ireland (AGAGE, <http://agage.mit.edu/>), instead.

160 N₂O flux density (F_{N_2O} , in $\mu\text{mol m}^{-2} \text{d}^{-1}$) was calculated as:

$$161 \quad F_{N_2O} = k_{N_2O} \times (N_{2O_{obs}} - N_{2O_{eq}}) \quad (2)$$

162 where k_{N_2O} (in cm h^{-1}) is the gas transfer velocity calculated with the method given by
163 Nightingale et al. (2000), as a function of the wind speed and the Schmidt number (Sc). The wind
164 speed data were obtained from the Kiel Lighthouse (see: www.geomar.de/service/wetter/), which
165 is approximately 20 km away from the BE Time-Series Station. The wind speed was normalized
166 to 10 m (u_{10}) to calculate k_{N_2O} (Hsu et al., 1994). k_{N_2O} was adjusted by multiplying with $(Sc/600)^{0.5}$,
167 and Sc was computed as:

$$168 \quad Sc = v/D_{N_2O} \quad (3)$$

$$169 \quad D_{N_2O} = 3.16 \times 10^{-6} e^{-18370/RT} \quad (4)$$

170 where v is the kinematic viscosity of seawater, which is calculated from the empirical equations
171 given in Siedler and Peters (1986), and D_{N_2O} is the diffusion coefficient of N₂O in seawater. R is
172 the universal gas constant and T is the water temperature in K.

173 **3. Result and discussion**

174 **3.1 Overview**

175 N₂O concentrations at the BE Time-Series Station showed significant temporal and depth-
176 dependent variations from 2005 to 2017 (Fig. 2). N₂O concentrations fluctuated between 1.2 and
177 37.8 nM, with an overall average of 13.9 ± 4.2 nM. This value was higher than the results from

178 the surface water of Station ALOHA ($5.9\text{--}7.4\text{ nmol kg}^{-1}$, average $6.5\pm 0.3\text{ nmol kg}^{-1}$, Wilson et
179 al., 2017), which is reasonable considering the weak anthropogenic impact in the North Pacific
180 Subtropical Gyre. The N_2O concentrations at BE were much lower than those measured at the
181 time-series station in the coastal upwelling area off Chile ($2.9\text{--}492\text{ nM}$, average $39.4\pm 29.2\text{ nM}$ in
182 the oxyclines and $37.6\pm 23.3\text{ nM}$ in the bottom waters, Farías et al., 2015) and a quasi-time series
183 station off Goa (Naqvi et al., 2010), where significant N_2O accumulations were observed in
184 subsurface waters at both locations. Our measurements were comparable to the time-series
185 station from Saanich Inlet ($\sim 0.5\text{--}37.4\text{ nM}$, average 14.7 nM , Capelle et al., 2018), a seasonally
186 anoxic fjord which has similar hydrographic conditions as BE.

187 NO_2^- concentrations fluctuated between below detection limit of $0.1\text{ }\mu\text{M}$ and $1.6\text{ }\mu\text{M}$, with an
188 average of $0.2\pm 0.3\text{ }\mu\text{M}$. NO_3^- concentrations varied from below detection limit of $0.3\text{ }\mu\text{M}$ to 17.9
189 μM , with an average of $2.0\pm 2.8\text{ }\mu\text{M}$. The temporal and spatial distributions of nitrite (NO_2^-) and
190 nitrate (NO_3^-) were similar during 2005–2017. A clear O_2 seasonality can be seen with severe O_2
191 depletion in the bottom waters during summer and autumn. Anoxia with the presence of H_2S
192 were detected in September/October 2005, September 2007, September/October 2014, and
193 September–November 2016. All of the extremely low N_2O concentrations ($<5\text{ nM}$) were
194 observed in the bottom waters in autumn, coinciding with hypoxia/anoxia, while the high N_2O
195 concentrations ($>20\text{ nM}$) sporadically occurred at different depths either in spring or autumn.

196 **3.2 Seasonal cycle**

197 Significant cycles at different frequencies were detected via wavelet analysis at the BE Time-
198 Series Station during 2005–2017 (Fig. 3). A half-year NO_2^- cycle sporadically occurred in 2007–
199 2009, 2013 and 2015. There is a seasonal NO_2^- variability (at the frequency of 1 year) between
200 2007 and 2016 (times before 2007 and after 2016 were outside the conic line), except during
201 2010–2012, when high NO_2^- concentrations were not observed in winter (Fig. 2). A biennial
202 cycle of NO_2^- could be observed as well during 2008–2015. The NO_3^- concentrations were
203 dominated by an annual cycle and a minor half-year cycle. The biennial cycle only occurred in
204 2008 and 2009. A remarkable seasonal variability of dissolved O_2 prevailed all the time, which is
205 also obvious from the times series data shown in Fig. 2. The annual N_2O cycle became gradually
206 more and more evident until 2014, then declined and reoccurred less intensely in 2016. The
207 periodical cycle was also present at other frequencies, indicated by the broadening of the red area
208 before 2015 in Fig. 2d. For example, a biennial N_2O cycle occurred during 2013–2015.

209 The half-year cycles of NO_2^- and NO_3^- were probably associated with algae blooms which
210 usually occur in each spring and autumn (Fig. S1 and S2). Since the time between the two
211 blooms differed between years, the cycles were weak and thus not present in every year. Due to
212 the fact that there was no half-year O_2 cycle at all, nutrients apart from O_2 might be the “drivers”
213 of the sporadic half-year N_2O cycle in 2008 and 2015, because N_2O production depends on the
214 concentration of the bioavailable nitrogen compounds (Codispoti et al., 2001).

215 Generally the wavelet analysis indicated a strong annual cycle for NO_2^- , NO_3^- , dissolved O_2 and
216 N_2O at the BE Time-Series Station, which enabled us to explore the seasonal pattern with annual
217 mean data. Although extreme values were excluded as a result of averaging, the smoothed results
218 generally reflect the seasonality of these parameters. Here, we focus on the annual cycle.

219 The annual mean vertical distribution of dissolved O_2 , NO_2^- , NO_3^- and N_2O are shown in Fig. 4.
220 Due to the development of stratification, the mixed layer was shallow in summer and deep in late
221 autumn/winter. O_2 depletion was observed in bottom waters from late spring until late autumn.
222 The seasonal variations of NO_2^- and NO_3^- were significantly correlated with each other
223 ($[\text{NO}_3^-]=11.59[\text{NO}_2^-]-0.51$, $R^2=0.80$, $n=72$, $p<0.0001$) and high concentrations were observed
224 for both in winter. Minimum N_2O concentrations were found in the bottom waters during
225 September and October, presumably as a result of consumption during denitrification under
226 anoxic condition (Codispoti et al., 2005). High N_2O concentrations were observed in late spring
227 and late autumn, respectively. In late spring N_2O accumulated in the bottom waters because the
228 stratification prevented mixing of the water column. In late autumn, however, N_2O could be
229 ventilated to the surface and thus emitted to the atmosphere due to the breakdown of the
230 stratification. The high N_2O concentrations could be attributed to enhanced N_2O production via
231 nitrification and/or denitrification within the oxic/anoxic interface (Goreau et al., 1980;
232 Codispoti et al., 1992). Since there is no clear O_2 concentration threshold, N_2O production from
233 both nitrification and the onset of denitrification overlap at oxic/anoxic interface. To this end,
234 direct N_2O production measurements (i.e. nitrification/denitrification rates) are required to
235 decipher which process dominates the formation of the different N_2O maxima.

236 High N_2O concentrations prevailed all over the water column in winter/early spring. NH_4^+ is
237 released from the sediment into bottom waters due to the degradation of organic matter,
238 especially after the autumn algae bloom (Fig. S1 and S2). The stratification usually completely
239 breaks down at this time of the year and the water column becomes oxygenated. Denitrification
240 is inhibited by the presence of high concentrations of dissolved O_2 ($> 20 \mu\text{mol L}^{-1}$, which is
241 higher than the O_2 threshold of about $10 \mu\text{mol L}^{-1}$, Tiedje, 1988) and thus nitrification is
242 presumably responsible for the high N_2O concentrations in winter/early spring.

243 **3.3 Trend analysis**

244 The MKTs were conducted for the surface (1m) and bottom (25m) N_2O concentrations and
245 saturations of the individual 12 months, respectively. Significant decreasing trends were detected
246 for the concentrations in the bottom waters for February and August (Table 1a), and for the
247 saturations in the surface for September and in the bottom for August and November (Table 1b).
248 These results indicated that some systematical changes in N_2O took place at BE. For example,
249 the significant decrease in N_2O concentration/saturation in August might be associated with the
250 increasing temperature, which reinforces the stratification and accelerates O_2 consumption in the
251 bottom waters (Lennartz et al., 2014). As a result, hypoxia/anoxia starts earlier and thus enables

252 the onset of denitrification to consume N₂O. During most of the months, trends in N₂O
253 concentration and saturation were not significant during 2005–2017.

254 A significant nutrient decline has been observed at the BE Time-Series Station since the mid-
255 1980s, however, Lennartz et al. (2014) found that bottom O₂ concentrations were still decreasing
256 over the past 60 years. The ongoing oxygen decline was attributed to the temperature-enhanced
257 O₂ consumption in the bottom water (Meier et al., 2018) and a prolongation of the stratification
258 period at the BE Time-Series Station (Lennartz et al., 2014). Please note that the trends in
259 nutrients and O₂ concentrations were detected based on the data collection which lasted for
260 approximately 30 and 60 years, respectively, while the N₂O observations at BE Time-Series
261 Station has lasted for only 12.5 years. Further MKT analysis for nutrients, temperature and
262 oxygen for months with significant trends in N₂O concentrations did not show any significant
263 results ($p > 0.05$). The significant trends in N₂O concentrations thus do not seem to be directly
264 related to one of these parameters, and we cannot state a reason for the significant trends of N₂O
265 concentration in February and the N₂O saturation in September and November at this point.
266 Presumably, a longer monitoring period for N₂O is required to detect corresponding trends in
267 N₂O and oxygen or nutrients.

268 **3.4 Extreme events**

269 **3.4.1 Low N₂O concentrations during October 2016-April 2017**

270 Besides the low N₂O concentrations occurring in autumn, we observed a band of pronounced
271 low N₂O concentrations which started in October 2016 and lasted until April 2017 (Fig. 5). In
272 this period N₂O concentrations varied between 5.5–13.9 nM, with an average of 8.4 ± 2.0 nM.
273 This is approximately 40% lower than the average N₂O concentration during the entire
274 measurement period 2005–2017. The average N₂O saturation during 2005–2017 was $111 \pm 30\%$,
275 while from October 2016 to April 2017, the N₂O saturations were as low as 43–93% (average
276 $62 \pm 10\%$).

277 Undersaturated N₂O waters have been previously reported from the Baltic Sea: Rönner (1983)
278 observed a N₂O surface saturation of 79% in the central Baltic Sea and attributed the
279 undersaturation to upwelling of N₂O-depleted waters. Bange et al. (1998) found a minimum N₂O
280 saturation of 91% in the southern Baltic Sea where the hydrographic conditions were
281 significantly influenced by riverine runoff. Walter et al. (2006) reported a mean N₂O saturation
282 of $79 \pm 11\%$ for shallow stations (<30 m) in the southwestern Baltic Sea in October 2003. The
283 low-N₂O event at BE was unusual because the concentrations were much lower than those
284 reported values and it lasted for more than half a year.

285 Although the observed temperatures and salinities during October 2016–April 2017 were
286 comparable to other years (Fig. S1), it is difficult to evaluate the role of physical mechanism in
287 the low-N₂O event because of insufficient data for water mass exchange at the BE Time-Series

288 Station. Here we mainly focused on the chemical or biological processes. Anoxia events with the
289 presence of H₂S were observed in the bottom waters for three months in a row during
290 September–November 2016. This is an unusual long period and is unprecedented at the BE
291 Time-Series Station. In December 2016 the stratification did not completely break down.
292 Although the water column was generally oxygenated, bottom O₂ concentrations were the lowest
293 observed during the past ten years. Considering the classical view of N₂O consumption via
294 denitrification under hypoxic and anoxic conditions, we inferred that denitrification accounted
295 for low N₂O concentrations in the bottom layer. However, the question still remains where the
296 low-N₂O-concentration water in the upper layers came from.

297 In September 2016, low N₂O concentrations were only observed in the bottom waters where the
298 anoxia occurred. However, the situation was different in the following months. During
299 October/November 2016, N₂O concentrations were homogeneously distributed in the water
300 column. Although the stratification gradually started to break down in late autumn, the density
301 gradient was still strong enough to keep the bottom waters at anoxic conditions and prevented
302 the low-N₂O-concentration to reach the surface. Thus we inferred that the unusual low N₂O
303 concentrations in the upper layers (above 20 m) were probably resulting from advection of
304 adjacent waters. Due to the fact that the upper layers were well-mixed and oxygenated, in situ
305 N₂O consumption in the water column could be neglected. We suggest therefore, that the N₂O
306 depleted waters were resulting from consumption of N₂O in bottom waters elsewhere and then
307 they were upwelled and transported to BE. Hence, N₂O consumption via denitrification might
308 have been, directly or indirectly, responsible for the low N₂O concentrations during October–
309 November 2016.

310 In December 2016, the bottom waters were ventilated with O₂. Although N₂O consumption by
311 denitrification should have been inhibited by the high concentrations of O₂ (Codispoti et al.,
312 2001), the N₂O concentrations did not restore to their normal level under suboxic conditions.
313 Since January 2017, the whole water column was well mixed and oxygenated. Usually a
314 significant nutrient supply could be observed starting in November (Fig. 4) as a result of
315 remineralization and vertical mixing, but the average NO₂⁻ and NO₃⁻ concentrations during
316 November 2016–April 2017 were 0.2 and 1.4 μM, respectively, which was about 50% and 60%
317 lower than in other years. Ammonium (NH₄⁺) and chlorophyll *a* concentrations during this
318 period were comparable to that of other years (Fig. S1). Secchi depth, a proxy of water
319 transparency, was 3.8 m in March 2017, which is only slightly lower compared to the monthly
320 average value for March (4.5±1.8 m). There is no exceptional spring algae bloom and thus we
321 infer that assimilative uptake of nutrients by phytoplankton was not responsible for the low
322 nutrients concentrations. The nutrient deficiency might be attributed to enhanced nitrogen
323 removal processes like denitrification or anammox (Voss et al., 2005; Hietanen et al., 2007;
324 Hannig et al., 2007) during the prolonged period of anoxia in autumn 2016. During the low N₂O
325 event, we found that N₂O concentrations were positively correlated with both NO₂⁻
326 ([N₂O]=7.02[NO₂⁻]+7.36, R²=0.29, n=24, p<0.01) and NO₃⁻ ([N₂O]=0.80[NO₃⁻]+7.36, R²=0.51,

327 n=24, $p < 0.0001$). These results indicate that the development and maintenance of the low-N₂O-
328 concentration was closely associated with nutrient deficiency. Especially after the breakdown of
329 the stratification, when denitrification was no longer a significant N₂O sink, nutrients might have
330 become a limiting factor for N₂O production.

331 In general, the low-N₂O-concentration event during October 2016–April 2017 can be divided
332 into two parts: in the stratified waters during October–November 2016, O₂ played a dominant
333 role and N₂O was consumed via denitrification under anoxic conditions. In the well-mixed water
334 column during December 2016–April 2017, nutrient deficiency seemed to have constrained N₂O
335 production via nitrification under suboxic/oxic conditions.

336 In recent years a novel biological N₂O consumption pathway, called N₂O fixation, which
337 transforms N₂O into particulate organic nitrogen via its assimilation, has been reported (Farías et
338 al., 2013). This process can take place under extreme environmental conditions even at very low
339 N₂O concentrations. Cornejo et al. (2015) reported that N₂O fixation might play a major role in
340 the coastal zone off central Chile where seasonally occurring surface N₂O undersaturation was
341 observed. The relatively high N₂ fixation rates in the Baltic Sea (Sohm et al., 2011) highlight the
342 potential role of N₂O fixation (Farías et al., 2013). However, we cannot quantify the role of
343 biological N₂O fixation for the N₂O depletion in the Baltic Sea due to the absence of N₂O
344 assimilation measurements.

345 **3.4.2 High N₂O concentrations in November 2017**

346 High N₂O concentrations were observed at the BE Time-Series Station in November 2017. The
347 average value reached 35.4 ± 1.5 nM, which was the highest concentration measured during the
348 entire sampling period from 2005 to 2017. Dissolved N₂O was homogeneously distributed in the
349 water column, but this event did not last long. In December, dissolved N₂O returned to normal
350 levels and the average concentration in the water column was comparable to that of other years.
351 Average N₂O saturation in November 2017 was $322 \pm 10\%$, which was also the highest for the
352 past 12.5 years. This value was much higher than the maximum surface N₂O saturation reported
353 by Rönner (1983) in the central Baltic Sea, but was comparable to the results observed in the
354 southern Baltic Sea (312%, Bange et al., 1998). Bange et al. (1998) linked the enhanced N₂O
355 concentrations to riverine runoff because those samples were collected in an estuarine area,
356 however, the riverine influence around the BE Time-Series Station is negligible. As a result, the
357 impact of fresh water input can be excluded.

358 Dissolved O₂ seemed to play a dominant role in the high N₂O concentrations. Enhanced N₂O
359 production usually occurred at the oxic/anoxic interface, which was closely linked to the
360 development of water column stratification. In general the breakdown of the stratification is
361 faster than its establishment at the BE Time-Series Station. As a result, it took about half a year
362 for bottom O₂ saturation to gradually decrease from ~80% to almost 0% (i.e. anoxia), but only
363 two months to restore normal saturation level in 2010 (Fig. 6). In late autumn, surface water

364 penetrated into the deep layers via vertical mixing and eroded the oxic/anoxic interface. The
365 entire water column quickly became oxygenated and the enhanced N₂O production was stopped.

366 Hypoxia/anoxia at BE is usually observed in the bottom waters in autumn, but in September
367 2017, hypoxic water (O₂ saturation < 20 %, which was close to the criterion for hypoxia, see
368 Naqvi et al., 2010) was found in the subsurface layer (10 m) as well. Surface O₂ saturation was
369 only ~50%, which was the lowest during the sampling period 2005–2017. The density gradient
370 of the water column in September 2017 was much lower than in other years. These results
371 indicate the occurrence of an upwelling event at BE Time-Series Station in autumn 2017, which
372 might be a result of the saline water inflow from the North Sea considering the change of salinity
373 in the water column (Fig. S1). Strong vertical mixing has interrupted the hypoxia/anoxia and
374 bottom O₂ saturation reached ~60% in October 2017. The presence of O₂ prevented N₂O
375 consumption via denitrification, as a result, we did not observe a significant N₂O decline during
376 that period (Fig. 5).

377 Considering the fact that a significant autumn algae bloom was observed in autumn 2017 (as
378 indicated by high chlorophyll a concentrations, see Fig. S1), severe O₂ depletion in the bottom
379 water could be expected. Although the bottom O₂ saturation was only slightly lower in
380 November than in October, we speculate that even lower O₂ saturation (but not anoxia) might
381 have occurred between October and November. The “W-shaped” O₂ saturation curve (see Fig. 6)
382 suggests that the stratification did not completely break down in October and that there might
383 have been a reestablishment of the oxic/anoxic interface providing favorable conditions for
384 enhanced N₂O production. Due to the degradation of organic nitrogen, NH₄⁺ is released from the
385 sediment into bottom waters (Dale et al., 2011), especially in autumn when O₂ is low (Fig. S2).
386 NH₄⁺ concentrations in November 2017 were lower than in other years (Fig. S1), and NO₂⁻
387 concentrations were higher (Fig. 5), indicating that nitrification occurred in bottom waters. To
388 this end, we suggest that the reestablishment of the oxic/anoxic interface promoted ammonium
389 oxidation (the first step of nitrification). In this case, N₂O could have temporarily accumulated
390 because its consumption via denitrification was blocked. Meanwhile, the relatively low density
391 gradient (i.e. low stratification) allowed upward mixing of the excess N₂O to the surface.
392 However, we inferred that that this phenomenon would only last for a few days due to the rapid
393 breakdown of stratification at the BE Time-Series Station.

394 Due to the development of the pronounced stratification, the oxic/anoxic interface prevailed in
395 summer/early autumn as well, but we did not observe N₂O accumulation during these months.
396 One of the potential explanations is that enhanced N₂O production only took place within
397 particular depths where strong O₂ gradient existed, but our vertical sampling resolution was too
398 low to capture this event. Also enhanced N₂O production might be covered by the weak mixing
399 which brought low-N₂O water from the bottom to the surface.

400 The upwelling event played different roles in autumn 2016 and 2017. First, upwelling took place
401 somewhere else but at BE because of the strong density and O₂ gradient in the water column

402 during autumn 2016. Second, bottom water remained anoxic in autumn 2016, while the
403 compensated water for upwelling in 2017 penetrated through stratification and brought O₂ into
404 bottom water (Fig. 6), which caused enhanced N₂O production. Similarly, autumn upwelling was
405 detected in 2011 and 2012 when we found relatively low O₂ concentrations in subsurface layers
406 (10 m) (Fig. 2), but we did not observe an increase in bottom O₂ concentrations and N₂O
407 concentrations remained low during that time. These upwelling events seem to be driven by
408 saline water inflow considering the prominent increase in salinity, but the mechanism dominates
409 O₂ input into bottom water before the stratification break down remains unclear.

410 **3.5 Flux density**

411 During 2005–2017, surface N₂O saturations at the BE Time-Series Station varied from 56 % to
412 314 % (69–194 % excluding the extreme values discussed in Sect. 3.4), with an average of
413 111±30 % (111±20 % without the extreme values). Generally the water column at BE was
414 slightly oversaturated with N₂O. Our results are in good agreement with the estimated mean
415 surface N₂O saturation for the European shelf (113%, Bange, 2006).

416 We found a weak seasonal cycle for surface N₂O concentrations, with high N₂O concentrations
417 occurring in winter/early spring and low concentrations occurring in summer/autumn, but no
418 such cycle for N₂O saturation (Fig. 4; Fig. 7). The seasonality in concentration but not in
419 saturation could be largely attributed to the effect of temperature on N₂O solubility: In summer
420 when surface N₂O concentrations are low, N₂O saturations are increased by the relative high
421 temperature; and vice versa in winter. Although salinity also affects N₂O solubility, its
422 contribution is negligible compared to temperature. Temperature alleviated the fluctuation of
423 surface N₂O saturation and thus affected the sea-to-air N₂O fluxes. We conclude that temperature
424 plays a modulating role for N₂O emissions.

425 The wind speed (u_{10}) at the BE Time-Series Station ranged from 1.1 to 14.0 m s⁻¹, with an
426 average of 7.0±2.7 m s⁻¹. N₂O flux densities varied from -19.0 to 105.7 μmol m⁻² d⁻¹ (-14.1–30.3
427 μmol m⁻² d⁻¹ without the extreme values), with an average of 3.5±12.4 μmol m⁻² d⁻¹ (3.3±6.5
428 μmol m⁻² d⁻¹ without the extreme values). However, the true emissions might have been
429 underestimated because our monthly sampling resolution is insufficient to capture short-term
430 N₂O accumulation events due to the fast breakdown of stratification in autumn. The uncertainty
431 introduced in the flux density computation was estimated to be 20% (Wanninkhof, 2014). The
432 flux densities at the BE Time-Series Station are comparable to those reported by Bange et al.
433 (1998, 0.4–7.1 μmol m⁻² d⁻¹) from the coastal waters of the southern Baltic Sea, but are slightly
434 lower than the average N₂O flux density reported by Rönner (1983, 8.9 μmol m⁻² d⁻¹) from the
435 central Baltic Sea. Please note that the results of Rönner (1983) were obtained only from the
436 summer season and therefore are probably biased because of missing seasonality.

437 In December 2014, a strong saline water inflow from the North Sea was observed, which was the
438 third strongest ever recorded (Mohrholz et al., 2015). Although the salinity in December 2014

439 was comparable to other years, a remarkable increase in salinity was observed in the following
440 several months. However, we did not detect a significant N₂O anomaly or enhanced emission
441 during that time. Similarly, Walter et al. (2006) investigated the impact of the North Sea water
442 inflow on N₂O production in the southern and central Baltic Sea in 2003. The oxygenated water
443 ventilated the deep Baltic Sea and shifted anoxic to oxic condition which led to enhanced N₂O
444 production, but the accumulated N₂O was unlikely to reach the surface due to the presence of a
445 permanent halocline (Walter et al., 2006).

446 Although we observed extremely high N₂O flux density in November 2017, the low-N₂O-
447 concentration (<10 nM) events have become more and more frequent during the past ten years
448 (Fig. 2). This phenomenon seldom occurred before 2011, but remarkable low N₂O
449 concentrations can be seen in 2011 and 2013, and to a less extent in 2012 and 2014. Similar
450 events lasted for several months in 2015 and for even more than half a year during 2016–2017.
451 The most striking was that the low-N₂O-concentration water was not only detected in bottom
452 waters, but also at surface which would significantly impact the air-sea N₂O flux densities.
453 Although the MKT result did not give a significant trend for the N₂O flux densities, the data
454 presented in Fig. 8 suggest a potential decline of N₂O flux densities from the coastal Baltic Sea,
455 challenging the conventional view that N₂O emissions from coastal waters would most probably
456 increase in the future, which was based on the hypothesis of increasing nutrient loads into coastal
457 waters. Due to an effective reduction of nutrient inputs, the severe eutrophication condition in the
458 Baltic Sea has been alleviated (HELCOM, 2018b), but ongoing deoxygenation points to the fact
459 that it will take a longer time for coastal ecosystems to feedback to reduced nutrient inputs
460 because other environmental changes such as warming may override decreasing eutrophication
461 (Lennartz et al., 2014).

462 **4. Conclusions**

463 The seasonal and inter-annual N₂O variations at the BE Time-Series Station from July 2005 to
464 December 2017 were driven by the prevailing O₂ regime and nutrients availability. We found a
465 pronounced seasonal cycle with low N₂O concentrations (undersaturations) occurring in
466 hypoxic/anoxic bottom waters in autumn and enhanced concentrations (supersaturations) all over
467 the water column in winter/early spring. Significant decreasing trends for N₂O concentrations
468 were found for few months, while most of the year, no significant trend was detectable in the
469 period of 2005–2017. During 2005–2017, no significant trends were present for O₂ and nutrients
470 either, but these parameters all show significant decreasing trends on longer time scales (~60
471 years) at BE. Our results show the strong coupling of N₂O with O₂ and nutrient concentrations,
472 and suggest similar changes on comparable time scales. Further monitoring of N₂O at BE time
473 series station is thus important to detect changes. Further studies on N₂O
474 production/consumption by nitrification and denitrification and analysis of the characteristic N₂O
475 isotope signature might be very helpful to decipher the potential roles of O₂/nutrients for N₂O
476 cycling.

477 Temperature plays a modulating role for the N₂O emission at the BE Time-Series Station.
478 Although the hydrographic condition at BE is generally dominated by the inflow of saline North
479 Sea water, this did not affect N₂O production and its emissions to the atmosphere. It seems that
480 events with extremely low N₂O concentrations and thus reduced N₂O emissions became more
481 frequent in recent years. Our results provide a new perspective onto potential future patterns of
482 N₂O distribution and emissions in coastal areas. Continuous measurement at the BE Time-Series
483 Station with a focus on late autumn would be of great importance for monitoring and
484 understanding the future changes of N₂O concentrations and emissions in the southwestern Baltic
485 Sea.

486 **Data availability**

487 Data are available from the Boknis Eck Database: www.bokniseck.de

488 **Author contribution**

489 X.M., S.T.L. and H.W.B. designed the study and participated in the fieldwork. N₂O
490 measurements and data processing were done by X.M. and S.T.L. X.M. wrote the manuscript
491 with contributions from S.T.L. and H.W.B.

492 **Competing interests**

493 The authors declare that they have no conflict of interest.

494 **Acknowledgments**

495 The authors thank the captain and crew of the RV *Littorina* and *Polarfuchs* as well as the many
496 colleagues and numerous students who helped with the sampling and measurements of the BE
497 time-series through various projects. Special thanks to A. Kock for her help with sampling,
498 measurements and data analysis. The time-series at BE was supported by DWK
499 Meeresforschung (1957–1975), HELCOM (1979–1995), BMBF (1995–1999), the Institut für
500 Meereskunde (1999–2003), IfM-GEOMAR (2004–2011) and GEOMAR (2012–present). The
501 current N₂O measurements at BE are supported by the EU BONUS INTEGRAL project which
502 receives funding from BONUS (Art 185), funded jointly by the EU, the German Federal
503 Ministry of Education and Research, the Swedish Research Council Formas, the Academy of
504 Finland, the Polish National Centre for Research and Development, and the Estonian Research
505 Council. The Boknis Eck Time-Series Station (www.bokniseck.de) is run by the Chemical
506 Oceanography Research Unit of GEOMAR, Helmholtz Centre for Ocean Research Kiel. Data
507 from BE are available from www.bokniseck.de/database-access. The N₂O data presented here
508 have been archived in MEMENTO (the MarinE MethanE and NiTrous Oxide database:
509 <https://memento.geomar.de>). X. Ma is grateful to the China Scholarship Council for providing
510 financial support (File No. 201306330056) and the EU BONUS INTEGRAL project.

511 **References**

- 512 Bange, H. W.: Nitrous oxide and methane in European coastal waters, *Estuar. Coast. Shelf S.*, 70,
513 361–374, <https://doi.org/10.1016/j.ecss.2006.05.042>, 2006.
- 514 Bange, H. W., Dahlke, S., Ramesh, R., Meyer-Reil, L. A., Rapsomanikis, S., and Andreae, M. O.:
515 Seasonal study of methane and nitrous oxide in the coastal waters of the southern Baltic Sea,
516 *Estuar. Coast. Shelf S.*, 47, 807–817, <https://doi.org/10.1006/ecss.1998.0397>, 1998.
- 517 Battaglia, G. and Joos, F.: Marine N₂O emissions from nitrification and denitrification
518 constrained by modern observations and projected in multimillennial global warming simulations,
519 *Global Biogeochem. Cy.*, 32, 92–121, <https://doi.org/10.1002/2017GB005671>, 2018.
- 520 Bonin, P., Gilewicz, M., and Bertrand, J. C.: Effects of oxygen on each step of denitrification on
521 *Pseudomonas nautica*, *Can. J. Microbiol.*, 35, 1061–1064, <https://doi.org/10.1139/m89-177>, 1989.
- 522 Breitburg, D., Levin, L. A., Oschlies, A., Grégoire, M., Chavez, F. P., Conley, D. J., Garçon, V.,
523 Gilbert, D., Gutiérrez, D., Isensee, K., Jacinto, G. S., Limburg, K. E., Montes, I., Naqvi, S. W. A.,
524 Pitcher, G. C., Rabalais, N. N., Roman, M. R., Rose, K. A., Seibel, B. A., Telszewski, M.,
525 Yasuhara, M., and Zhang, J.: Declining oxygen in the global ocean and coastal waters, *Science*,
526 359, eaam7240, <http://dx.doi.org/10.1126/science.aam7240>, 2018.
- 527 Capelle, D. W., Hawley, A. K., Hallam, S. J., and Tortell, P. D.: A multi-year time-series of N₂O
528 dynamics in a seasonally anoxic fjord: Saanich Inlet, British Columbia, *Limnol. Oceanogr.*, 63,
529 524–539, <https://doi.org/10.1002/lno.10645>, 2018.
- 530 Carstensen, J., Andersen, J. H., Gustafsson, B. G., and Conley, D. J.: Deoxygenation of the
531 Baltic Sea during the last century, *P. Natl. Acad. Sci. USA*, 111, 5628–5633,
532 <https://doi.org/10.1073/pnas.1323156111>, 2014.
- 533 Codispoti, L. A., Elkins, J. W., Yoshinari, T., Fredrich, G., Sakamoto, C., and Packard, T.: On
534 the nitrous oxide flux from productive regions that contain low oxygen waters, in: *Oceanography*
535 *of the Indian Ocean*, edited by Desai, B. N., Oxford Univ. Press, New York, 271–284, 1992.
- 536 Codispoti, L. A., Brandes, J. A., Christensen, J. P., Devol, A. H., Naqvi, S. W. A., Paerl, H. W.,
537 and Yoshinari, T.: The oceanic fixed nitrogen and nitrous oxide budgets: Moving targets as we
538 enter the anthropocene? *Sci. Mar.*, 65, 85–105, <https://doi.org/10.3989/scimar.2001.65s285>, 2001.
- 539 Codispoti, L. A., Yoshinari, T., and Devol, A. H.: Suboxic respiration in the oceanic water
540 column, in: *Respiration in aquatic ecosystems*, edited by del Giorgio, P. A. and Williams, P. J.,
541 Oxford Univ. Press, New York, 225–247, 2005.

542 Conley, D. J., Carstensen, J., Aigars, J., Axe, P., Bonsdorff, E., Eremina, T., and Lannegren, C.:
543 Hypoxia is increasing in the coastal zone of the Baltic Sea, *Environ. Sci. Technol.*, 45, 6777–
544 6783, doi: 10.1021/es201212r, 2011.

545 Cornejo, M., Murillo, A. A., and Farías, L.: An unaccounted for N₂O sink in the surface water of
546 the eastern subtropical South Pacific: Physical versus biological mechanisms, *Prog. Oceanogr.*,
547 137, 12–23, <https://doi.org/10.1016/j.pocean.2014.12.016>, 2015.

548 Dale, A. W., Sommer, S., Bohlen, L., Treude, T., Bertics, V. J., Bange, H. W., Pfannkuche, O.,
549 Schorp, T., Mattsdotter, M., and Wallmann, K.: Rates and regulation of nitrogen cycling in
550 seasonally hypoxic sediments during winter (Boknis Eck, SW Baltic Sea): Sensitivity to
551 environmental variables, *Estuar. Coast. Shelf S.*, 95, 14–28,
552 <https://doi.org/10.1016/j.ecss.2011.05.016>, 2011.

553 Ducklow, H. W., Doney, S. C., and Steinberg, D. K.: Contributions of long-term research and
554 time-series observations to marine ecology and biogeochemistry, *Annu. Rev. Mar. Sci.*, 1, 279–
555 302, <https://doi.org/10.1146/annurev.marine.010908.163801>, 2009.

556 Farías, L., Castro-González, M., Cornejo, M., Charpentier, J., Faúndez, J., Boontanon, N., and
557 Yoshida, N.: Denitrification and nitrous oxide cycling within the upper oxycline of the eastern
558 tropical South Pacific oxygen minimum zone, *Limnol. Oceanogr.*, 54, 132–144,
559 <https://doi.org/10.4319/lo.2009.54.1.0132>, 2009.

560 Farías, L., Faúndez, J., Fernández, C., Cornejo, M., Sanhueza, S., and Carrasco, C.: Biological
561 N₂O fixation in the Eastern South Pacific Ocean and marine cyanobacterial cultures, *Plos one*, 8,
562 e63956, <https://doi.org/10.1371/journal.pone.0063956>, 2013.

563 Farías, L., Besoain, V., and García-Loyola, S.: Presence of nitrous oxide hotspots in the coastal
564 upwelling area off central Chile: an analysis of temporal variability based on ten years of a
565 biogeochemical time series, *Environ. Res. Lett.*, 10, 044017, doi:10.1088/1748-
566 9326/10/4/044017, 2015.

567 Goreau, T. J., Kaplan, W. A., Wofsy, S. C., McElroy, M. B., Valois, F. W., and Watson, S.W.:
568 Production of NO₂⁻ and N₂O by nitrifying bacteria at reduced concentrations of oxygen, *Appl.*
569 *Environ. Microb.*, 40, 526–532, 1980.

570 Grasshoff, K., Kremling, K., and Ehrhardt, M.: *Methods of seawater analysis*, 3rd edition,
571 WILEY-VCH, Weinheim, Germany, 1999.

572 Hannig, M., Lavik, G., Kuypers, M. M. M., Woebken, D., Martens-Habbena, W., and Jürgens,
573 K.: Shift from denitrification to anammox after inflow events in the central Baltic Sea, *Limnol.*
574 *Oceanogr.*, 52, 1336–1345, 2007.

575 Hansen, H. P., Giesenhausen, H. C., and Behrends, G.: Seasonal and long-term control of bottom
576 water oxygen deficiency in a stratified shallow-coastal system, *ICES J. Mar. Sci.*, 56, 65–71, doi:
577 10.1006/jmsc.1999.0629, 1999.

578 HELCOM: Sources and pathways of nutrients to the Baltic Sea, *Baltic Sea Environ. Proc.*, 153,
579 2018a.

580 HELCOM: State of the Baltic Sea - Second HELCOM holistic assessment 2011–2016, *Baltic*
581 *Sea Environ. Proc.*, 155, <http://stateofthebalticsea.helcom.fi/>, 2018b.

582 Hietanen, S., and Lukkari, K.: Effects of short-term anoxia on benthic denitrification, nutrient
583 fluxes and phosphorus forms in coastal Baltic sediment, *Aquat. Microb. Ecol.*, 49, 293–302,
584 <https://doi.org/10.3354/ame01146>, 2007.

585 Hsu, S. A., Meindl, E. A., and Gilhousen, D. B.: Determining the power-law wind-profile
586 exponent under near-neutral stability conditions at sea, *J. Appl. Meteorol.*, 33, 757–765,
587 [https://doi.org/10.1175/1520-0450\(1994\)033<0757:DTPLWP>2.0.CO;2](https://doi.org/10.1175/1520-0450(1994)033<0757:DTPLWP>2.0.CO;2), 1994.

588 IPCC: Climate Change 2013: The physical science basis. Contribution of Working Group I to the
589 fifth assessment report of the Intergovernmental Panel on Climate Change, Cambridge
590 University Press, Cambridge, UK and New York, NY, 2013.

591 Landolfi, A., Somes, C. J., Koeve, W., Zamora, L. M., and Oschlies, A.: Oceanic nitrogen
592 cycling and N₂O flux perturbations in the Anthropocene, *Global Biogeochem. Cy.*, 31, 1236–
593 1255, doi:10.1002/2017GB005633, 2017.

594 Lennartz, S. T., Lehmann, A., Herrford, J., Malien, F., Hansen, H. P., Biester, H., and Bange, H.
595 W.: Long-term trends at the Boknis Eck time series station (Baltic Sea), 1957–2013: does
596 climate change counteract the decline in eutrophication? *Biogeosciences*, 11, 6323–6339,
597 <https://doi.org/10.5194/bg-11-6323-2014>, 2014.

598 Löscher, C. R., Kock, A., Könneke, M., LaRoche, J., Bange, H. W., and Schmitz, R. A.:
599 Production of oceanic nitrous oxide by ammonia-oxidizing archaea, *Biogeosciences*. 9, 2419–
600 2429, <https://doi.org/10.5194/bg-9-2419-2012>, 2012.

601 Kock, A., Arévalo-Martínez, D. L., Löscher, C. R., and Bange, H. W.: Extreme N₂O
602 accumulation in the coastal oxygen minimum zone off Peru, *Biogeosciences*. 13, 827–840, doi:
603 10.5194/bg-13-827-2016, 2016.

604 Kroeze, C., and Seitzinger, S. P.: Nitrogen inputs to rivers, estuaries and continental shelves and
605 related nitrous oxide emissions in 1990 and 2050: a global model, *Nutr. Cycl. Agroecosys.*, 52,
606 195–212, 1998.

607 Kulkarni, A., and Von Storch, H.: Monte Carlo experiments on the effect of serial correlation on
608 the Mann-Kendall test of trend, *Meteorol. Z.*, 4, 82–85, 1995.

609 Martinez-Rey, J., Bopp, L., Gehlen, M., Tagliabue, A., and Gruber, N.: Projections of oceanic
610 N₂O emissions in the 21st century using the IPSL Earth system model, *Biogeosciences*, 12,
611 4133–4148, doi: 10.5194/bg-12-4133-2015, 2015.

612 Meier, H. M., Väli, G., Naumann, M., Eilola, K., and Frauen, C.: Recently accelerated oxygen
613 consumption rates amplify deoxygenation in the Baltic Sea, *J. Geophys. Res.-Oceans.*, 123,
614 3227–3240, <https://doi.org/10.1029/2017JC013686>, 2018.

615 Mohrholz, V., Naumann, M., Nausch, G., Krüger, S., and Gräwe, U.: Fresh oxygen for the Baltic
616 Sea-An exceptional saline inflow after a decade of stagnation, *J. Marine Syst.*, 148, 152-166,
617 <https://doi.org/10.1016/j.jmarsys.2015.03.005>, 2015.

618 Naqvi, S. W. A., Jayakumar, D. A., Narvekar, P. V., Naik, H., Sarma, V. V. S. S., D'souza, W.,
619 Joseph, S., and George, M. D.: Increased marine production of N₂O due to intensifying anoxia
620 on the Indian continental shelf, *Nature*, 408, 346, 2000.

621 Naqvi, S.W.A., Bange, H.W., Farías, L., Monteiro, P.M.S., Scranton, M.I., and Zhang, J.: Marine
622 hypoxia/anoxia as a source of CH₄ and N₂O, *Biogeosciences*, 7, 2159–2190,
623 <https://doi.org/10.5194/bg-7-2159-2010>, 2010.

624 Nevison, C., Butler, J. H., and Elkins, J. W.: Global distribution of N₂O and the ΔN₂O-AOU
625 yield in the subsurface ocean, *Global Biogeochem. Cy.*, 17,
626 <https://doi.org/10.1029/2003GB002068>, 2003.

627 Nightingale, P., G. Malin, C. S. Law, A. J. Watson, P. S. Liss, M. I. Liddicoat, J. Boutin, and R.
628 C. Upstill-Goddard: In situ evaluation of air-sea gas exchange parameterizations using novel
629 conservative and volatile tracers, *Global Biogeochem. Cy.*, 14, 373–387,
630 <https://doi.org/10.1029/1999GB900091>, 2000.

631 Rabalais, N. N., Cai, W.-J., Carstensen, J., Conley, D. J., Fry, B., Hu, X., Quinones-Rivera, Z.,
632 Rosenberg, R., Slomp, C. P., Turner, R. E., Voss, M., Wissel, B., and Zhang, J.: Eutrophication-
633 driven deoxygenation in the coastal ocean, *Oceanography*, 27, 172–183,
634 <https://doi.org/10.5670/oceanog.2014.21>, 2014.

635 Ravishankara, A. R., Danielm J., S., and Portmann, R. W.: Nitrous oxide (N₂O): the dominant
636 ozone-depleting substance emitted in the 21st century, *Science*, 326, 123–125, doi:
637 10.1126/science.1176985, 2009.

638 Rönner, U.: Distribution, production and consumption of nitrous oxide in the Baltic Sea,
639 *Geochim. Cosmochim. Ac.*, 47, 2179–2188, [https://doi.org/10.1016/0016-7037\(83\)90041-8](https://doi.org/10.1016/0016-7037(83)90041-8),
640 1983.

641 Schlittgen, R., and Streitberg, B. H. J.: *Zeitreihenanalyse*, Oldenburg Wissenschaftsverlag,
642 Munich, Germany, 2001.

643 Seitzinger, S. P., and Kroeze, C.: Global distribution of nitrous oxide production and N inputs in
644 freshwater and coastal marine ecosystems, *Global Biogeochem. Cy.*, 12, 93–113, 1998.

645 Siedler, G., and Peters, H.: Properties of sea water, in: *Oceanography*, edited by Sündermann J.,
646 Springer, Berlin, Heidelberg, 233–264, 1986.

647 Simone, F.: Mann-Kendall Test, MathWorks,
648 <https://ww2.mathworks.cn/matlabcentral/fileexchange/25531-mann-kendall-test>, 2009.

649 Sohm, J. A., Webb, E. A., and Capone, D. G.: Emerging patterns of marine nitrogen fixation, *Nat.*
650 *Rev. Microbiol.*, 9, 499–508, doi: 10.1038/nrmicro2594, 2011.

651 Tiedje, J. M.: Ecology of denitrification and dissimilatory nitrate reduction to ammonium, in:
652 *Environmental Microbiology of Anaerobes*, edited by: Zehnder, A. J. B., John Wiley & Sons,
653 N.Y., 179–244, 1988.

654 Torrence, C., and Compo, G. P.: A practical guide to wavelet analysis, *B. Am. Meteorol. Soc.*,
655 79, 61–78, [https://doi.org/10.1175/1520-0477\(1998\)079<0061:APGTWA>2.0.CO;2](https://doi.org/10.1175/1520-0477(1998)079<0061:APGTWA>2.0.CO;2), 1998.

656 Torrence, C., and Compo, G. P.: Wavelet analysis, <http://paos.colorado.edu/research/wavelets/>,
657 2004.

658 Voss, M., Emeis, K. C., Hille, S., Neumann, T., and Dippner, J. W.: Nitrogen cycle of the Baltic
659 Sea from an isotopic perspective, *Global Biogeochem. Cy.*, 19, doi: 10.1029/2004GB002338,
660 2005.

661 Walter, S., Breitenbach, U., Bange, H. W., Nausch, G., and Wallace, D. W.: Distribution of N₂O
662 in the Baltic Sea during transition from anoxic to oxic conditions, *Biogeosciences*, 3, 557–570,
663 <https://doi.org/10.5194/bg-3-557-2006>, 2006.

664 Wanninkhof, R.: Relationship between wind speed and gas exchange over the ocean revisited,
665 *Limnol. Oceanogr.: Methods*, 12, 351–362, <https://doi.org/10.4319/lom.2014.12.351>, 2014.

666 Weiss, R. F., and Price, B. A.: Nitrous oxide solubility in water and seawater, *Mar. Chem.*, 8,
667 347–359, [https://doi.org/10.1016/0304-4203\(80\)90024-9](https://doi.org/10.1016/0304-4203(80)90024-9), 1980.

668 Wilson, S. T., Ferrón, S., and Karl, D. M.: Interannual variability of methane and nitrous oxide in
669 the North Pacific Subtropical Gyre, *Geophys. Res. Lett.*, 44, 9885–9892,
670 <https://doi.org/10.1002/2017GL074458>, 2017.

671 Xu, Z. X., Takeuchi, K., and Ishidaira, H.: Monotonic trend and step changes in Japanese
672 precipitation, *J. Hydrol.*, 279, 144–150, [https://doi.org/10.1016/S0022-1694\(03\)00178-1](https://doi.org/10.1016/S0022-1694(03)00178-1), 2003.

673 Yang, D., Li, C., Hu, H., Lei, Z., Yang, S., Kusuda, T., Koike, T., and Musiaka, K.: Analysis of
674 water resources variability in the Yellow river of China during the last half century using the
675 historical data, *Water Resour. Res.*, 40, 1–12, <https://doi.org/10.1029/2003WR002763>, 2004.

676 Zhang, G.-L., Zhang, J., Liu, S.-M., Ren, J.-L., and Zhao, Y.-C.: Nitrous oxide in the Changjiang
677 (Yangtze River) estuary and its adjacent marine area: Riverine input, sediment release and
678 atmospheric fluxes, *Biogeosciences*, 7, 3505–3516, <https://doi.org/10.5194/bg-7-3505-2010>,
679 2010.

680 Table 1. The results of the Mann-Kendall test for the surface and bottom N₂O concentrations and
 681 saturations of the 12 individual months.

682 Table 1a. MKT results for N₂O concentrations

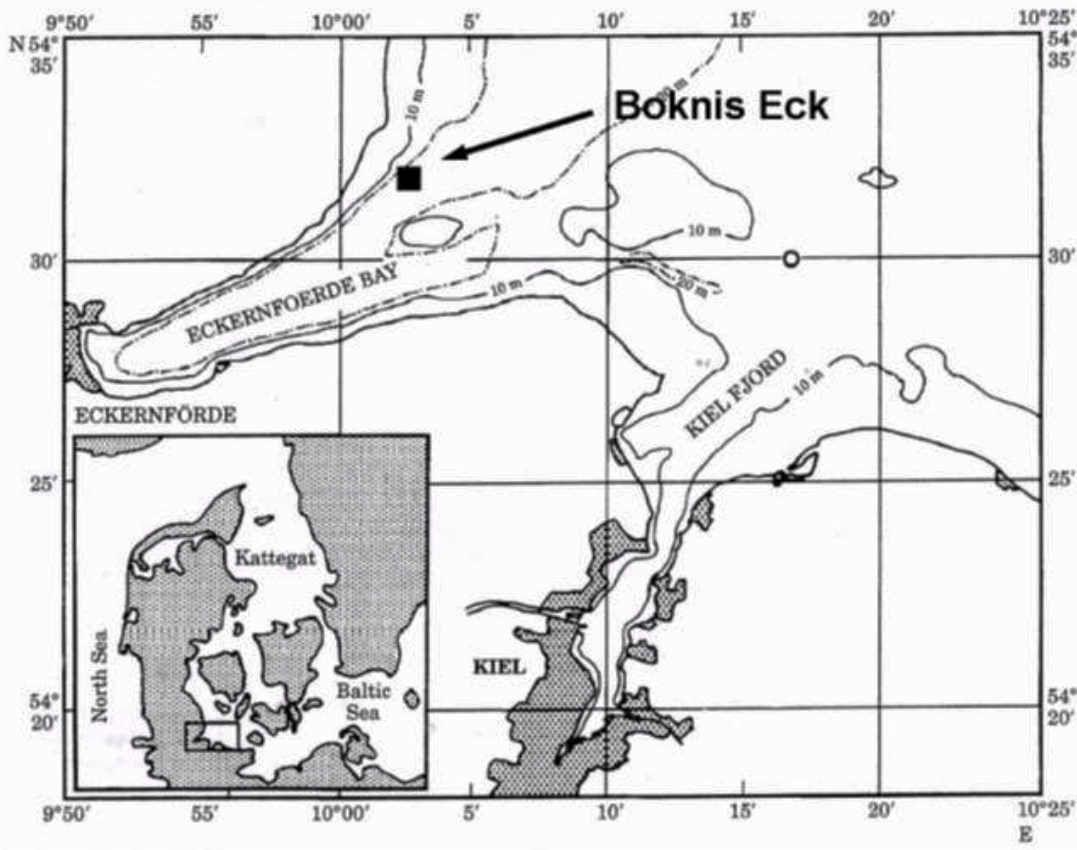
Month	January		February		March		April	
Depth/m	1	25	1	25	1	25	1	25
p	0.09	0.19	0.11	0.03(-)	0.19	0.63	0.09	0.30
Month	May		June		July		August	
Depth/m	1	25	1	25	1	25	1	25
p	0.63	0.24	0.15	0.95	0.16	0.16	0.20	0.03(-)
Month	September		October		November		December	
Depth/m	1	25	1	25	1	25	1	25
p	0.25	0.76	0.36	0.76	0.67	0.16	0.10	0.30

683

684 Table 1b. MKT results for N₂O saturations

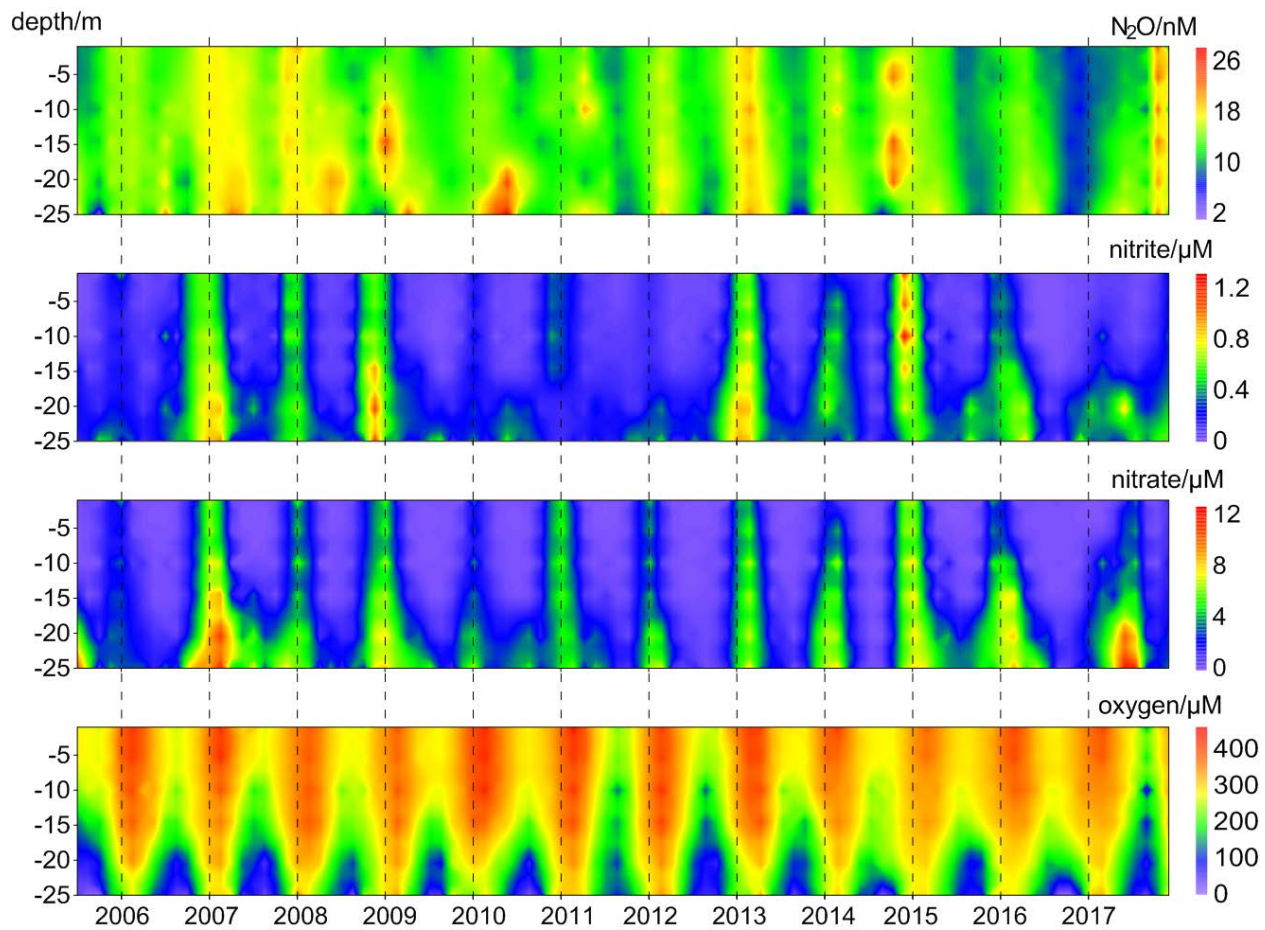
Month	January		February		March		April	
Depth/m	1	25	1	25	1	25	1	25
p	0.37	0.24	0.15	0.15	0.19	0.63	0.11	0.19
Month	May		June		July		August	
Depth/m	1	25	1	25	1	25	1	25
p	0.19	1	0.37	0.54	0.10	0.43	0.20	0.02(-)
Month	September		October		November		December	
Depth/m	1	25	1	25	1	25	1	25
p	0.04(-)	0.85	0.06	0.43	0.20	0.03(-)	0.16	0.36

685
 686 p indicates the p-value of the test, which is the probability, under the null hypothesis, of obtaining a value of
 687 the test statistic as extreme or more extreme than the value computed from the sample.
 688 (-) indicates a rejection of the null hypothesis at α significance level and a decreasing trend is detected.



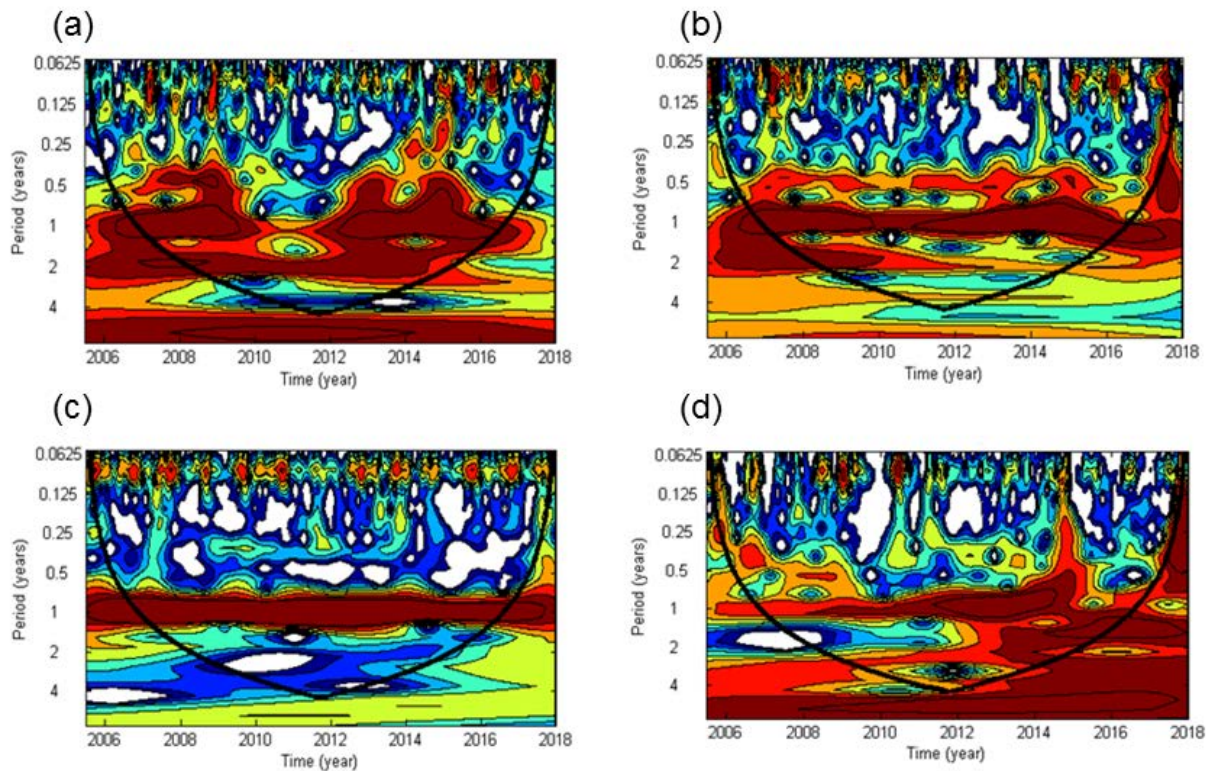
689

690 Fig. 1 Location of the Boknis Eck Time-Series Station in the Eckernförde Bay, southwestern Baltic Sea. (Map
 691 from Hansen et al., 1999)



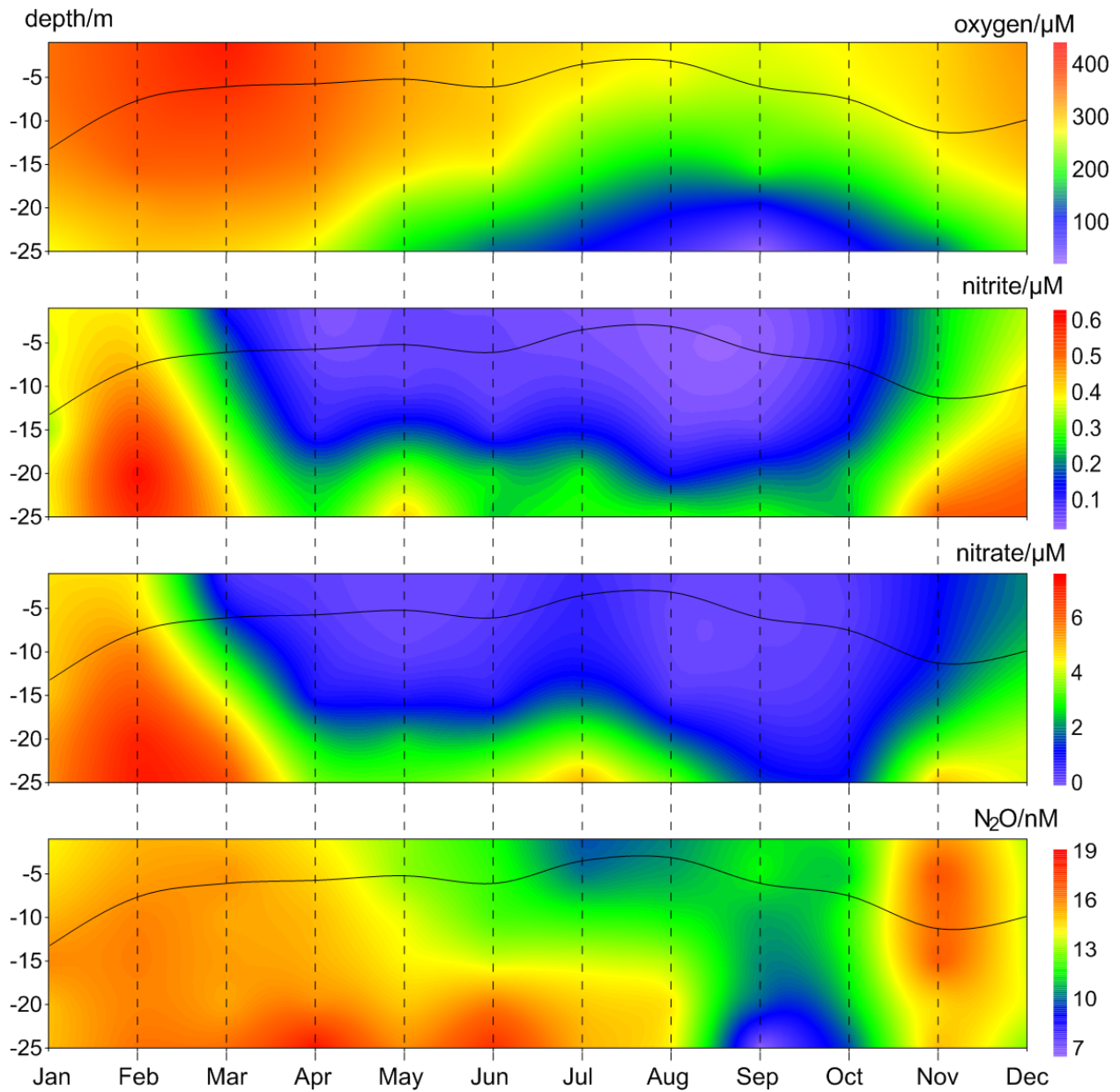
692

693 Fig. 2 Vertical distributions of dissolved O_2 , NO_2^- , NO_3^- , and N_2O from the BE Time-Series Station during
 694 2005–2017.



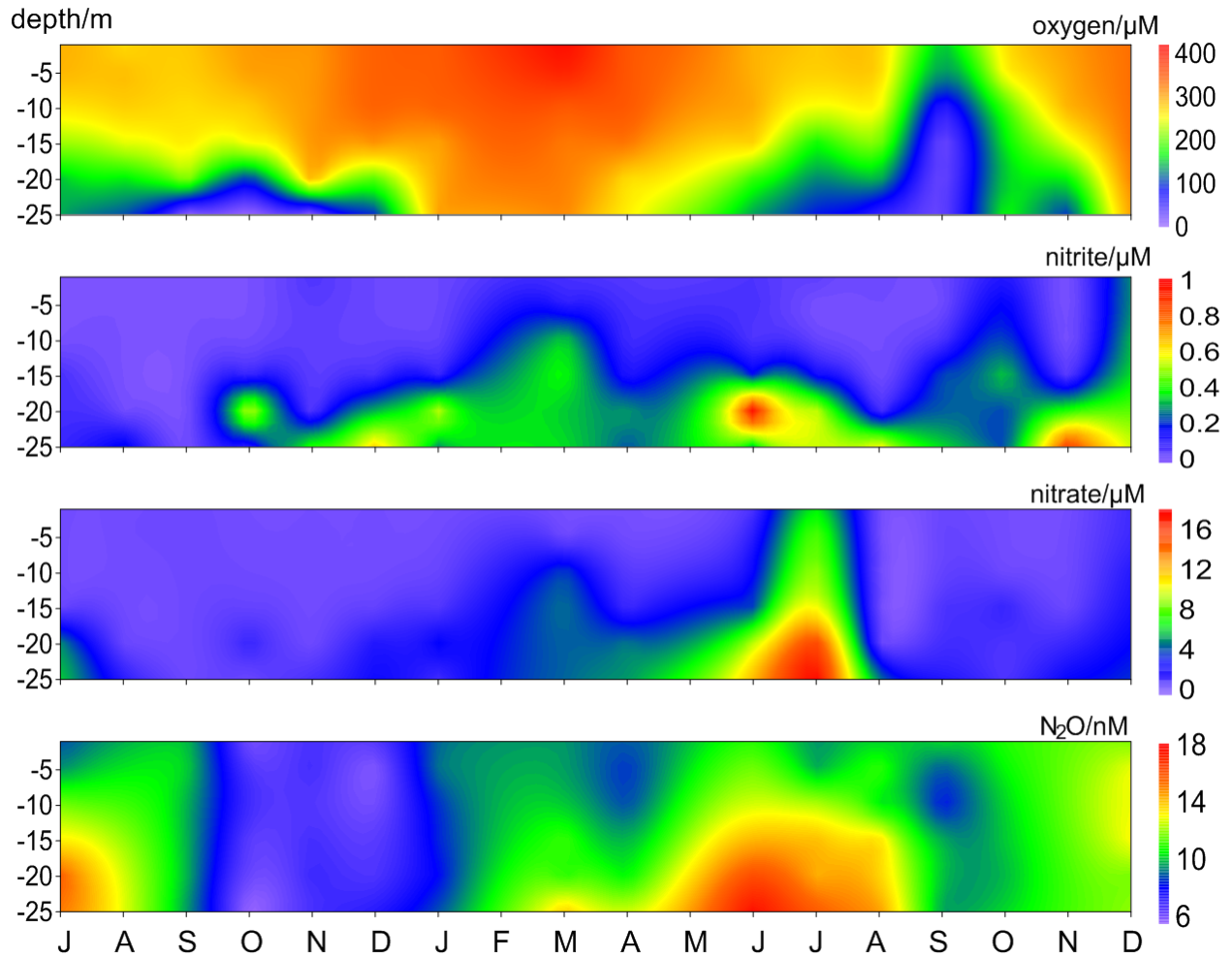
695

696 Fig. 3 Wavelet power spectra of NO_2^- (a), NO_3^- (b), dissolved O_2 (c) and N_2O (d) from the BE Time-Series
 697 Station. Red areas indicate high, blue indicate low power. The black conic line indicates the significant area
 698 where boundary effects can be excluded.

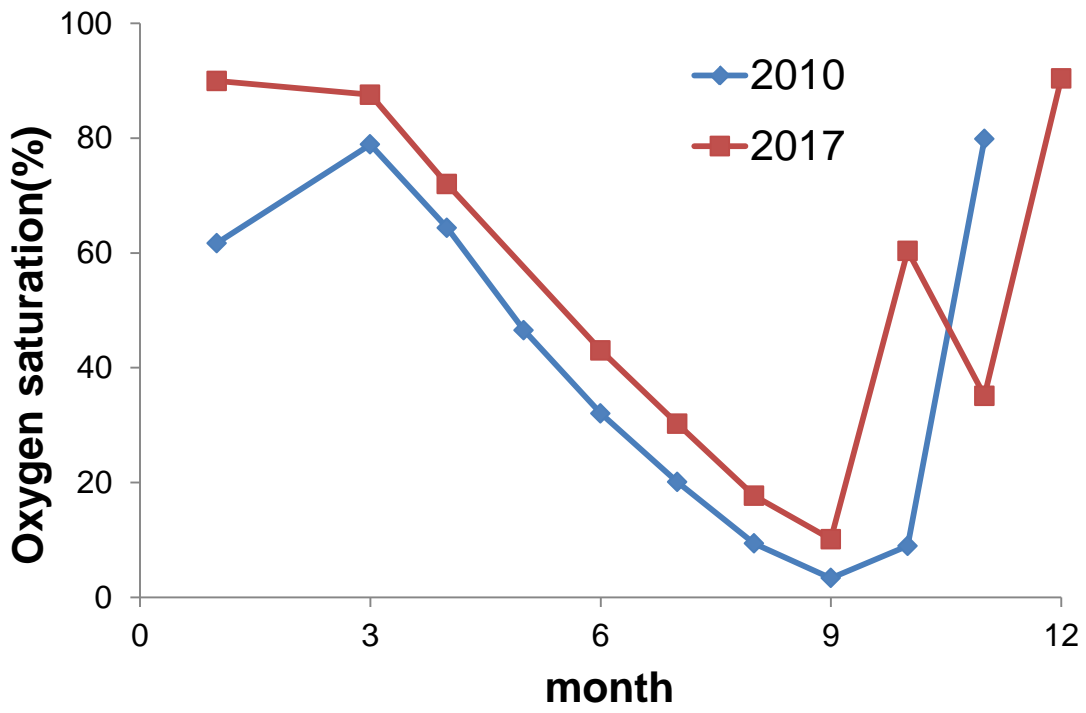


699

700 Fig. 4 Average vertical distributions of dissolved O_2 , NO_2^- , NO_3^- , and N_2O from the BE Time-Series Station
 701 during 2005–2017. The black line indicates the mixed layer depth, which was calculated based on a potential
 702 density anomaly of 0.15 kg m^{-3} from the sea surface (1m).

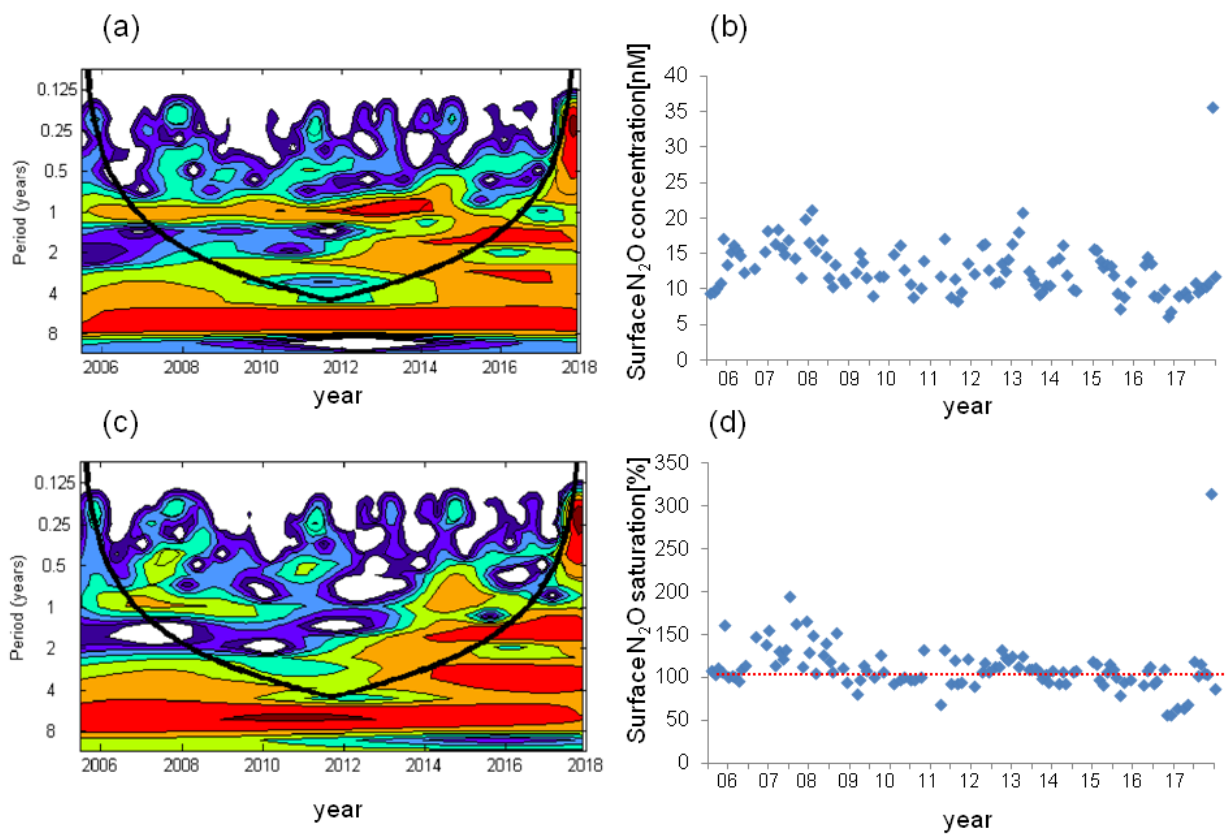


703
 704 Fig. 5 Vertical distribution of dissolved O_2 , NO_2^- , NO_3^- , and N_2O from the BE Time-Series Station during July
 705 2016–December 2017. Please note that the high N_2O concentrations in November 2017 were removed for
 706 better visualization.



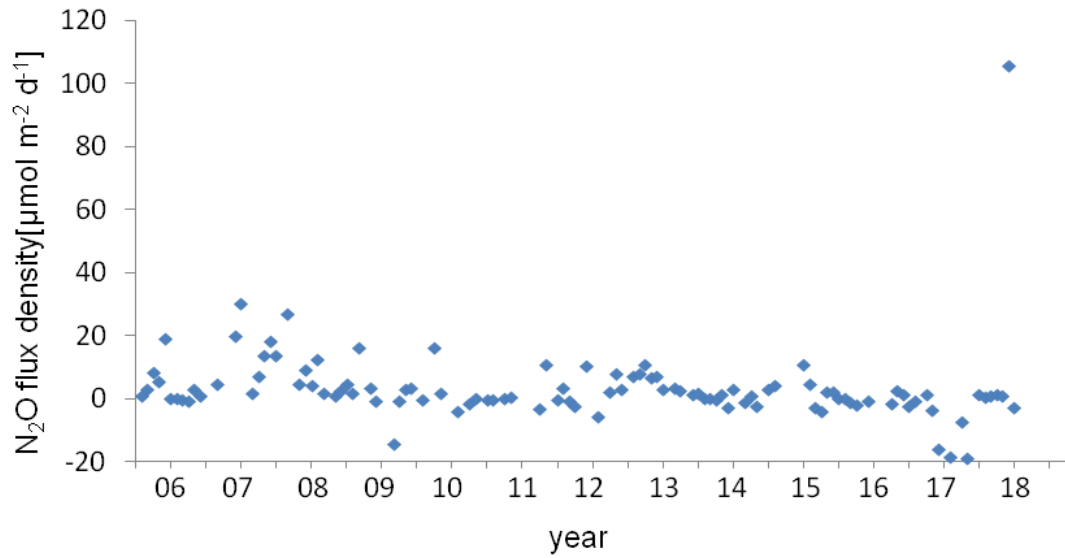
707

708 Fig. 6 Variations of bottom O₂ saturation in 2010 (blue) and 2017 (red).



709

710 Fig. 7 Wavelet analysis and the variation of surface N_2O concentrations (a, b) and surface N_2O saturations (c,
 711 d). The dashed red line in (d) indicates the saturation of 100%.



712

713 Fig. 8 Variation of N₂O flux density at the BE Time Series-Station during 2005–2017. Negative values
 714 indicated N₂O influx from the atmosphere and positive values indicated N₂O efflux to the atmosphere.